The Cold Spray Process and Its Potential for Industrial Applications

Frank Gärtner, Thorsten Stoltenhoff, Tobias Schmidt, and Heinrich Kreye

(Submitted July 29, 2005; in revised form January 19, 2006)

Cold spraying has attracted serious attention since unique coating properties can be obtained by the process that are not achievable by conventional thermal spraying. This uniqueness is due to the fact that coating deposition takes place without exposing the spray or substrate material to high temperatures and, in particular, without melting the sprayed particles. Thus, oxidation and other undesired reactions can be avoided. Spray particles adhere to the substrate only because of their high kinetic energy on impact. For successful bonding, powder particles have to exceed a critical velocity on impact, which is dependent on the properties of the particular spray material. This requires new concepts for the description of coating formation but also indicates applications beyond the market for typical thermal spray coatings. The present contribution summarizes the current "state of the art" in cold spraying and demonstrates concepts for process optimization.

1. Introduction

In thermal spraying, bonding between splats and the closing of pores can be enhanced by high temperatures or high particle velocities during particle impact. The thermal and kinetic energy contents of particles impinging the substrate vary from one process to another. However, for metallic materials or composites high process temperatures can increase the amount of oxides embedded in the coating and therefore reduce their performance in technical applications (Ref 1). In flame spraying or high-velocity oxy-fuel (HVOF) flame spraying, possible reactions of the feedstock material with the oxygen needed for combustion, with the combustion products, and with the oxygen in the air mixed into the free jet have to be considered as well as the oxidation of hot coating surfaces. In some cases, the reaction of the spray material with the ambient atmosphere can be reduced by shrouding the flame with an inert gas. Oxidation can also be limited for processes that do not require the presence of a combustion flame, like plasma spraying (PS) or arc spraying (AS), by using a controlled atmosphere in a closed chamber. However, the comparison of atmospheric PS and vacuum PS (VPS) has already shown that the latter can be performed only at significantly higher costs. Moreover, in comparison to processes operating in the ambient atmosphere, the application of VPS does not allow sufficient cooling of the base material, which therefore has to tolerate the effects of enhanced temperatures. These include

solid-state phase transformation and phase growth as well as the thermal distortion of complex components. Therefore, over the last two decades, the development of flame-based spray systems that work in ambient atmospheres has been aimed at reducing the temperature of particles and increasing their velocity (Fig. 1). In HVOF spraying, higher particle velocities were obtained by using converging-diverging de Laval-type nozzle designs and higher gas pressures. With a chamber pressure of up to 10 bar, HVOF spray systems of the third generation accelerate spray particles to velocities of about 650 m/s. Coating microstructures demonstrate that only small particles or fractions of larger ones are molten before the impact onto the substrate. A further reduction in particle temperatures below the melting temperatures of metals requires a substantial increase in velocity, which can only be realized by optimizing the expansion ratio in the diverging nozzle section and by using higher chamber pressures. Following an alternative concept working without plasma or flame, the development of cold spraying started about 20 years ago by a group of scientists at the Institute of Theoretical and Applied Mechanics, Novosibirsk, Russia (Ref 2-4). The process operates at high gas pressures of up to 30 bar and more and by electrical heating well adjustable low gas temperatures. As indicated in Fig. 1, ensuring very high particle velocities, cold spraying just fills the far edge of the above spectrum in the development of spray processes.

The general principle of cold spraying is sketched in Fig. 2 and has been described elsewhere in more detail (Ref 5-7). A high-pressure gas is preheated and led into a converging-diverging de Laval-type nozzle. The fluidized cold spray powder is fed axially and centrally into the nozzle. In the divergent section, gas and powder particles are accelerated to supersonic velocities and are cooled down to temperatures that are typically around room temperature or even lower. The characteristic dimensions of the nozzle are the throat diameter, the length of the divergent section, and the expansion ratio, which is given as the ratio between the cross section of the nozzle exit and the cross section of the nozzle throat.

Apart from these established descriptions, up to the present time a couple of slightly different layouts have also been prop-

Frank Gärtner, Thorsten Stoltenhoff, Tobias Schmidt, and **Heinrich Kreye,** Helmut Schmidt University, Hamburg, Germany. Contact e-mail: frank.gaertner@hsu-hh.de.
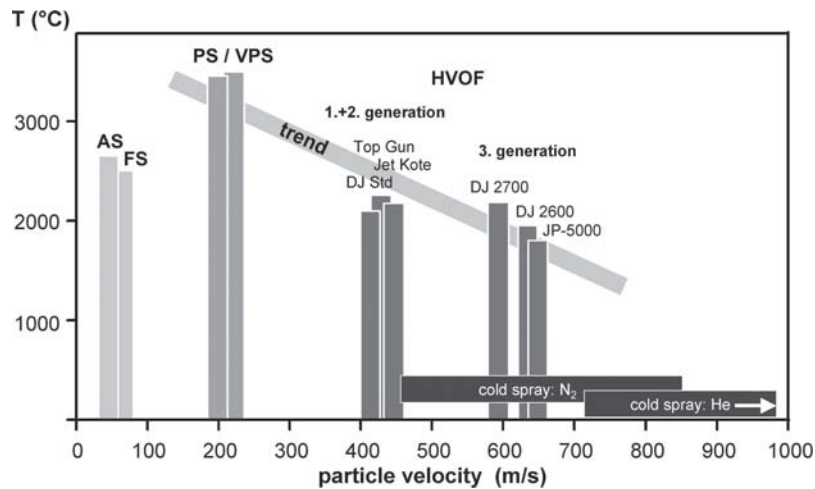
Fig. 1 Particle temperatures and velocities obtained in different thermal spray processes, as measured for high-density materials. The bar indicates the observed trend of recent developments.
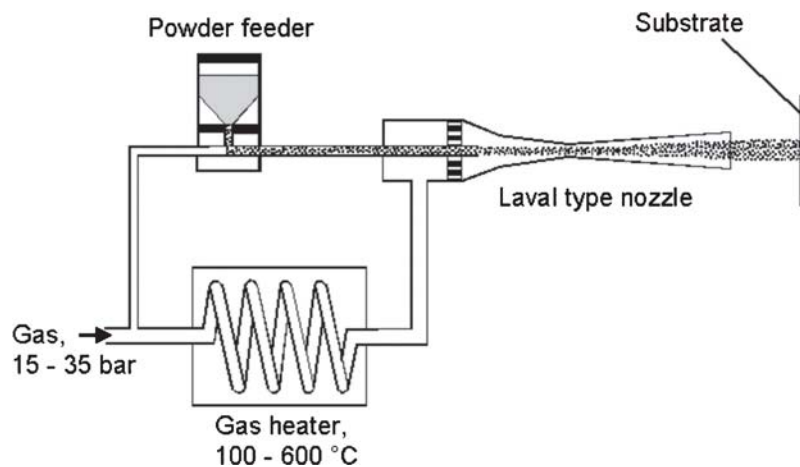

Fig. 2 Schematic of the cold spray process

agated by various groups of authors, claiming: (a) benefits by using smaller diameters of the smallest nozzle cross section, lower mass loads on powder feed lines, and larger powder size cuts (Ref 8, 9); (b) different powder injection schemes and the additional use of hard-phase particles to consolidate coatings (Ref 10); or (c) the use of small-diameter nozzles with only slightly diverging cross sections in the expanding regimen to compensate for the decrease in the sonic gas velocities caused by the friction at the nozzle wall (Ref 11). In addition to the above-mentioned layouts, a couple of pieces of individually designed cold-spray devices have been operating at universities or research centers. A couple of devices using modifications of the original design are running under different process descriptions, probably in an attempt to bypass the original patents by Alkhimov and colleagues (Ref 2, 3). It might be noted that from the physical point of view, coating formation by solid impact does not require different process descriptions.

As demonstrated by the fast increasing number of contributions to the annual meetings of the International Thermal Spray Society, cold spraying nowadays is attracting serious world-wide attention. Current studies on the topic are aimed at optimizing nozzle designs, exploring possible bonding mechanisms, or demonstrating the applicability of various spray materials. For a deeper understanding of the process, the relationships between the deposition efficiencies and particle velocity were investigated (Ref 5, 12, 13). As illustrated schematically in Fig. 3, particles impacting at low velocities will abrade the substrate material, whereas at higher velocities, deposition and coating formation can occur. These relationships lead to the postulation and evaluation of the critical particle velocity needed for bonding.

The ongoing research in the field of cold spraying has been aided by computational methods in fluid dynamics and in the thermomechanical modeling of particle impacts. While computational fluid dynamics (CFD) is being used with the aim of increasing the particle velocity (Ref 7, 14-16), the modeling of particle impact is used to provide a better understanding of the bonding mechanisms, and to estimate critical velocities for bonding particles of different materials (Ref 17, 18). By means of a so-far widely accepted model, bonding in cold spraying can
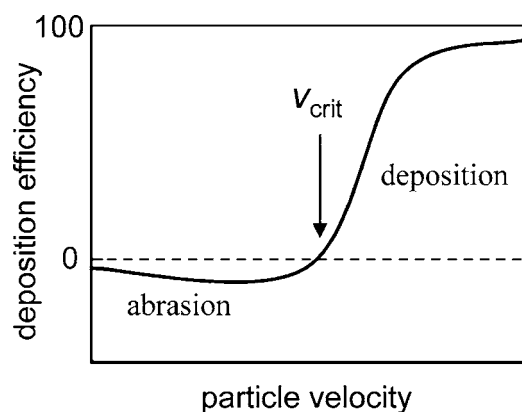
Fig. 3 Schematic of the correlation between particle velocity and deposition efficiency. The transition between abrasion in the low-velocity range and deposition for high velocities defines the critical velocity. V_{crit}, critical velocity.

be explained by the occurrence of local shear instabilities at particle-substrate and particle-particle interfaces due to thermal softening, as first shown by Assadi et al. (Ref 18). Later work was aimed at refining the procedures for calculation and its applications to different spray materials (Ref 19, 20). Based on the concept of bonding by shear instabilities and by combining the results from modeling and experimental investigations, analytical expressions were recently developed to predict the ranges of optimum spray conditions with respect to the mechanical properties of spray materials, spray particle sizes, and particle temperatures (Ref 21).
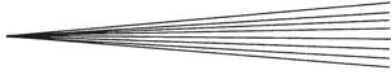
Another focus in cold spraying is the exploration of the feasibility of different feedstock materials. As shown in the latest proceedings of the International Thermal Spray Conference (ITSC) conferences, quite a number of investigations concern process development for standard engineering materials and deal with different aspects to customize cold spraying for various spray powders envisaging short-term applications. To demonstrate the versatility of the process, a couple of such examples are also given in the present article. With respect to powder developments, significant attention is being paid to new material types. It has been shown that cold spraying is suitable to process coatings on the basis of nanocrystalline alloys (Ref 22), nanocrystalline composites (Ref 23, 24), or bulk metallic glasses (Ref 25), just to mention a couple.

This article reports on the current "state of the art" in cold-spray process development. Taking the example of copper as the spray material, the influences of optimized spray conditions on coating quality are reported. With respect to the above-mentioned understanding of the process, special emphasis is given to current investigations to tune cold-spray parameters to different applications. The given examples of coating microstructures of various materials should demonstrate the versatility of the process.

2. Procedures

2.1 Determination of Critical Velocities

For a variety of spray materials, the critical velocity for successful impacts was determined by correlating the deposition

efficiency with the respective spray particle size distributions. A range of various deposition efficiencies were obtained by using different nozzle geometries (Ref 7) or by varying process parameters such as gas temperature and pressure (Ref 12). The present investigation is based on a method by which the effects of gas temperature are minimized by using the same parameter settings and different nozzle types (Ref 7). For each set of process conditions, particle velocity and temperature were calculated by using CFD. This approach assumes that the mechanical properties and the extent of oxidation are similar and independent of particle size for the particular feedstock powder.

2.2 Investigations of Coating Microstructures and Bond Strength

To evaluate coating quality with respect to porosity and the amount of well-bonded particle-particle interfaces, cross sections were subsequently prepared and investigated by optical microscopy. The microstructural features of embedded copper particles and particle-particle interfaces were revealed by chemical etching with a solution of 25 mL of H_2O, 25 mL of ammonia (25% in H_2O), and 5 ml of hydrogen peroxide (3% in H_2O). A selection of coating cross sections was further investigated by scanning electron microscopy.

Bond strength measurements were performed in a tensile mode according to the European standard EN582 (comparable to ASTM standard C 633-01; Ref 26). Before cold spraying, steel substrates were degreased and grit blasted. To avoid the thermal influences by preparation, the gluing of as-sprayed bond-strength samples to counterbodies was performed at 60 °C by using adhesive DP 490 (3M, St. Paul, MN). The oxygen contents of the initial feedstock and of the coatings were measured by using a commercial analyzer of the model TC300 type manufactured by LECO (St. Joseph, MI). The coatings were mechanically detached from the substrate by bending the substrate side of the flat coupons over a sharp edge with an radius of 5 mm, using a mechanical testing machine and a procedure similar to that in 3-point bending tests.

2.3 Nozzle Developments

By launching cold spraying, nozzle designs of a slightly trumpet-like shape were originally propagated (Ref 3, 5). Referring to radial symmetry, the smallest cross section of such a "standard" nozzle of a slightly trumpet-like shape has a width of 2.7 mm, a length of the diverging section of 70 mm, and an expansion ratio of 8.8. Using the numerical codes of fluid dynamics, gas and particle flow for certain process conditions were calculated (Ref 7). The numerical codes of fluid dynamics, in particular the method of characteristics (MOC), were also used to develop new nozzle designs that allow a more homogeneous particle acceleration (Ref 27).

3. Results and Discussion

3.1 Evaluation of Critical Velocities

In the high-velocity gas stream, smaller particles are accelerated to significantly higher velocities than large particles (Ref 7, 14). Only very small particles are subject to deceleration in the
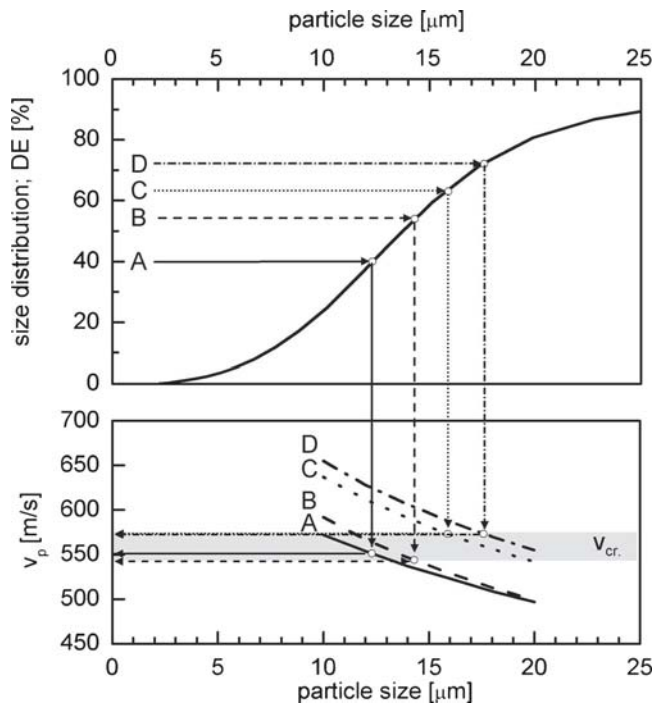
Fig. 4 Experimentally determined deposition efficiencies and cumulative particle size distribution as obtained for different nozzle types A, B, C, and D (indicated by arrows) in correlation with calculated individual particle velocities (process gas N$_2$; pressure 30 bar; temperature 300 °C). Nozzle A: trumpet shape; smallest diameter 2.7 mm; length of divergent section 70 mm; expansion ratio 5.8. Nozzle B: trumpet shape; smallest diameter 2.7 mm; length of divergent section 70 mm; expansion ratio 8.8 (standard nozzle). Nozzle C: bell shape; smallest diameter 2.7 mm; length of divergent section 100 mm; expansion ratio 5.8. Nozzle D: bell shape; smallest diameter 2.7 mm; length of divergent section 100 mm; expansion ratio 8.8. Under these process conditions, copper particles adhere at velocities of ~550 m/s.

stagnation area in front of the substrate. Experimental investigations show that particles with velocities lower than a specific critical velocity result in the erosion of coatings rather than in the building up of coatings. Particles with velocities above the critical limit, on the other hand, adhere to the substrate or coating. Since the velocity of a particle is a function of its size, the amount of adhering material can be correlated to the respective size distribution of a particular powder. The critical velocity for bonding is the velocity of the largest particle that bonds to the substrate. If the size cut of the powder contains only negligible amounts of fine particles, the cumulative size distribution can be correlated directly to the deposition efficiency in cold spraying (Ref 7). Figure 4 demonstrates the general procedure on the example of a spherical copper powder with particle sizes mainly between 5 and 25 μm and an oxygen content of smaller than 0.2%. To demonstrate the capability of this procedure, the critical velocity for that particular powder was measured by using different nozzle geometries. In these experiments, a unique set of spray parameters was used to avoid the influences of pressure or impact temperature. For four different nozzle geometries, Fig. 4 correlates the experimentally determined cumulative powder size distribution and deposition efficiencies with calculated individual particle velocities. Considering the possible er-
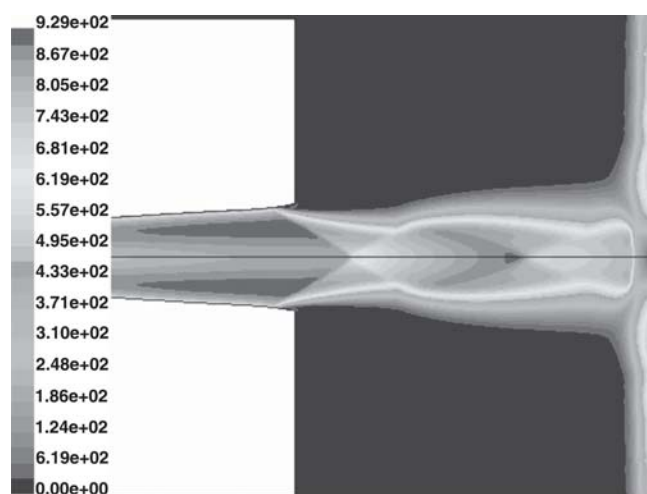
rors in determining the particle size distribution, a velocity of 550 m/s was worked out as the critical velocity for depositing that high-purity copper powder. In a similar way, critical velocities were determined for different spray materials, different powder sizes, and various impact temperatures. It is worth noting that one or two spray experiments should be sufficient to determine the critical velocities for a particular powder.
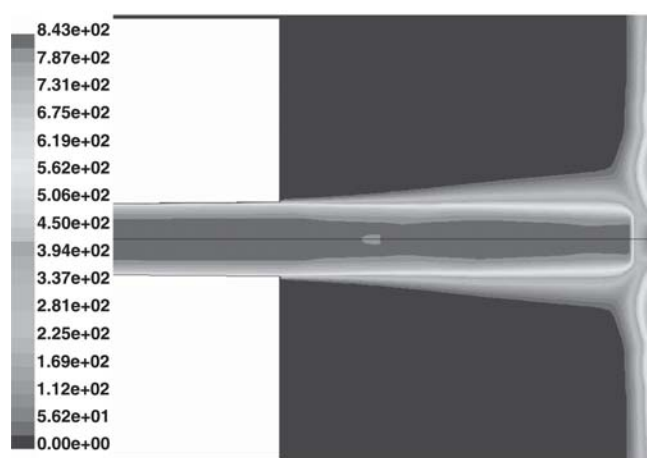
3.2 Process Improvements

Using the procedures of fluid dynamics, nozzle designs were developed that provide the maximum acceleration of feedstock particles for given spray materials and process gases. According to the MOC, the bell-shaped nozzle geometries can guarantee better and more homogeneous particle acceleration over the diameter of the nozzle cross section. The most influential parameter is the choice of process gas, resulting in different, optimum expansion ratios (Ref 27). For cold spraying copper and other feedstock powders of similar density with nitrogen as the process gas, keeping the width of the smallest cross section at 2.7 mm, calculations according to the MOC supplied a bell-shaped nozzle geometry (i.e., a MOC nozzle) with a length of 130 mm for the diverging cross section and an expansion ratio of 5.8. This type of nozzle is capable of also providing good coating qualities for a number of other spray materials.

In Fig. 5, the calculated flow fields of the free gas jets of a "standard" type nozzle and a nozzle designed by the MOC are compared. The velocity contours demonstrate that the velocity distribution at the exit of the MOC-designed nozzle is significantly more homogenous than that of the standard nozzle. Moreover, by the parallel gas stream of the bell-shaped MOC-designed nozzle, the occurrence of compression knots (shock diamonds) in the free jet can be suppressed to a remarkable degree, which cannot be obtained by using the standard trumpet-shaped nozzle. Both the more homogeneous velocity distribution and the higher gas velocities in the free jet contribute to a more efficient particle acceleration.

To illustrate the effect of nozzle geometries and process temperatures, the velocities of a copper particle with a diameter of 20 μm were calculated for using nitrogen as the process gas at a gas inlet pressure of 30 bar, which is the usual standard for the cold spraying of copper (Fig. 6). Using the standard trumpet-shaped nozzle and a gas inlet temperature of 320 °C, which so far serves as the standard gas temperature for spraying copper using a steel nozzle, the particle will be accelerated to a velocity of 500 m/s, which is not high enough to allow the bonding of copper. At the same parameter settings using the bell-shaped MOC-designed nozzle, the velocity of a 20 μm copper particle is increased to 580 m/s, which is well above the critical velocity of copper of 550 m/s. Developments in the manufacturing of cold spray nozzles on the basis of sintered hard metals can offer further advantages. For copper as spray feedstock, nozzle plugging can be avoided even at higher process gas temperatures by using WC-Co as the nozzle material. It must be stated that other feedstock materials, such as aluminum alloys, require particular tuning of the nozzle materials to avoid nozzle fouling (Ref 28). By using a WC-Co-based nozzle, copper can be sprayed with a gas inlet temperature of 600 °C, which increases the impact velocity of a 20 μm particle up to 670 m/s. This significant increase in particle velocities can enhance the applications for several rea-

Fig. 5 Velocity contours of the free gas jets at exits of (a) the trumpet-shaped, standard nozzle and (b) the optimized bell-shaped, MOC-designed nozzle.

Fig. 6 Calculated impact velocities of a 20 μm copper particle as function of gas inlet temperature for the trumpet-shaped standard nozzle and the bell-shaped MOC-designed nozzle. The arrows indicate the increase of attainable velocities by an optimized nozzle design and by using sintered WC-Co as the nozzle material.

Therefore, microstructural cross sections and analyses of oxygen content do not reveal internal, oxygen-rich layers after individual passes of the spray torch even by operating at higher temperatures (compare later Fig. 7 and 8).

3.3 Microstructures and Properties of Cold Sprayed Copper Coatings

With respect to different powder types, the necessary process conditions of cold spraying were evaluated by subsequent investigations of coating microstructures. Figure 7 shows micrographs of a typical copper coating on a copper substrate, which was sprayed with the standard trumpet-shaped nozzle, using a −25 + 5 μm powder. The coating was deposited by using a nitrogen inlet pressure of 30 bar and a gas temperature of 300 °C. Figure 7(a) demonstrates that such coatings can be processed with porosities of far less than 1%. The etching of sample cross sections can be tuned to reveal the internal grain boundaries of former spray particles. Such chemical attack would be too strong for more open defects. Particle-particle interfaces, which are held only by mechanical forces, would be over etched and appear dark in the optical micrograph. The close-up view of the etched cross section in Fig. 7(b) reveals grain boundaries inside the former spray particles and highly deformed grains close to particle-particle interfaces. In addition, a fairly high amount of ~30 to 40% of the overall particle-particle interface cuts appear in a similar contrast as normal grain boundaries.

In the as-sprayed state, the hardness of the cold-sprayed coatings, which were processed with a trumpet-shaped nozzle and using N_2 at 30 bar and 300 °C, corresponds to that of annealed and then heavily deformed bulk material that has been cold rolled to a 90% reduction in thickness (Table 1). On steel, cold-sprayed coatings obtain bond strengths of about 10 to 20 MPa, which are higher or similar to those of AS coatings (Table 1). Using aluminum as the substrate material, a significantly higher bond strength of more than 40 MPa was achieved. Such differences can probably be explained by experiments showing that

sons. First, with respect to standard conditions (i.e., trumpet-shaped nozzle, and N_2 used at a temperature of 320 °C), the deposition efficiency for using a standard cold spray powder (sizes of −25 + 5 μm) can be increased from 60% to more than 90%. Second, larger and therefore cheaper particle size cuts can be used in cold spraying. Since the critical velocity decreases with particle size (Ref 21), even larger particle size distributions of −38 + 10 μm can be sprayed with similar high deposition efficiencies of ~90%.

By increasing the process gas temperatures, the optical appearance of the coating surfaces changes color from copper-like to more pronounced red and brown tones at high gas inlet temperatures, but these thin layers have no effect on the oxide content of the copper coatings. Even for optimized nozzle designs, spray particles in the outer halo of the particle beam have lower velocities and thus abrade a thin layer of the substrate surface. By the traverse motion of the spray gun, the outer ring of the spray particle jet grit-blasts the substrate and, in an inert gas atmosphere, prepares fresh surfaces for further deposition.
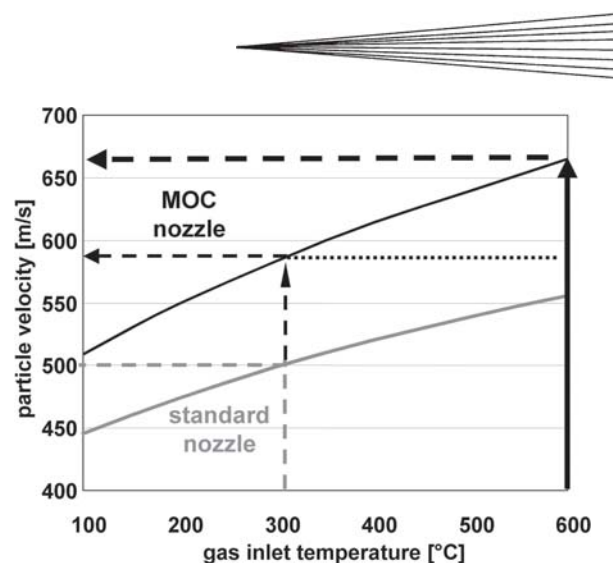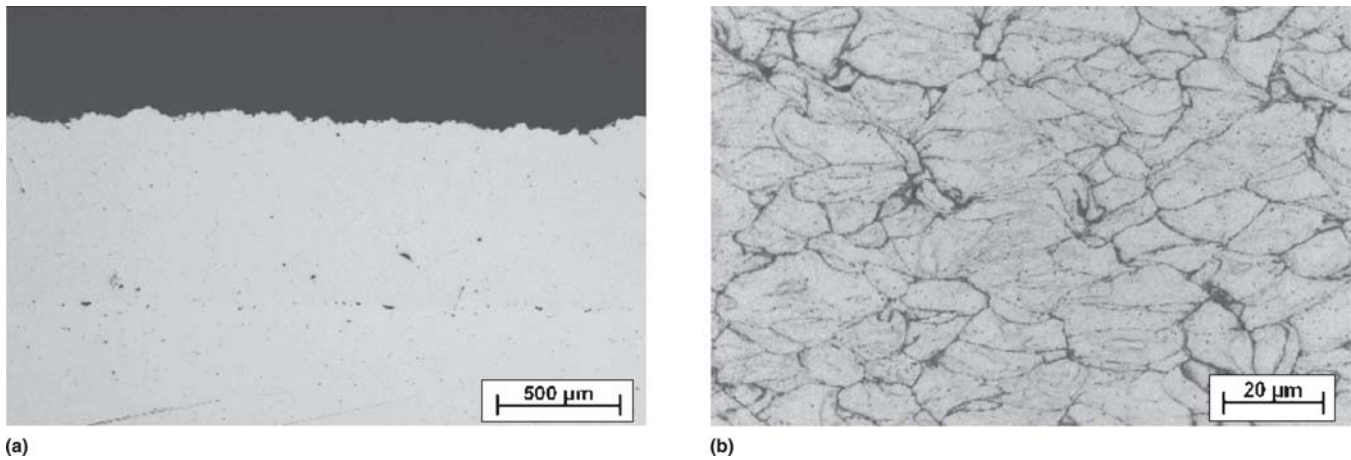
Fig. 7   Cu on Cu substrate cold sprayed with a trumpet-shaped standard nozzle (powder −22 + 5 µm; process gas N_2; temperature 320 °C; pressure 30 bar); (a) overview; (b) close-up. The close-up view of the etched cross section (b) reveals grain boundaries and particle-particle interfaces.
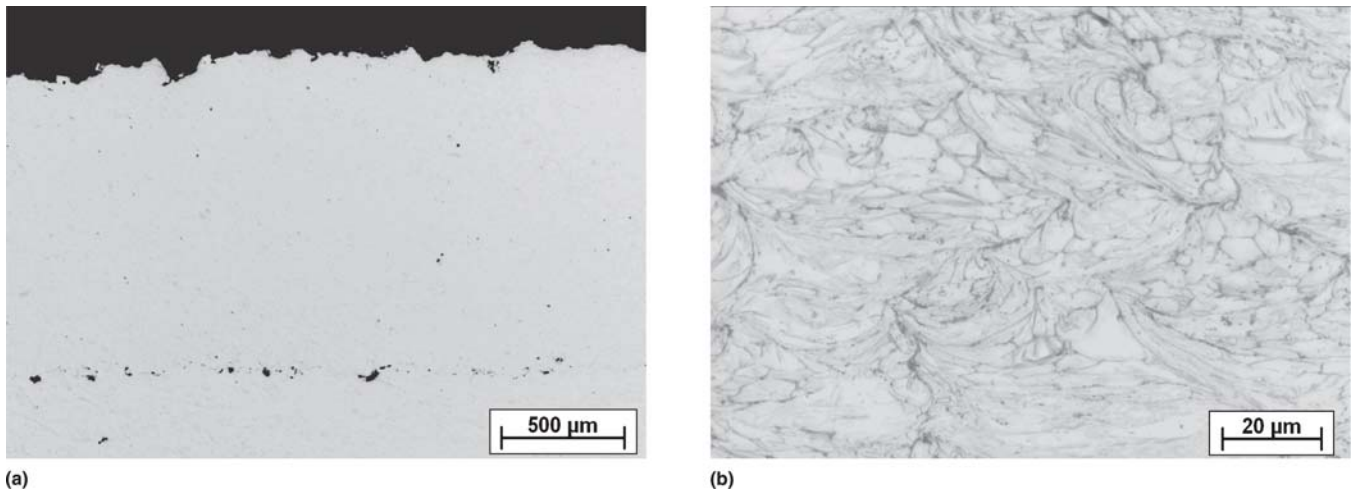

Fig. 8   Cu on Cu substrate cold sprayed with a bell-shaped MOC-designed nozzle (powder −38 + 10 µm; process gas N_2; temperature 500 °C; pressure 30 bar); (a) overview; (b) close-up.

Table 1   Key data and properties of cold-sprayed copper coatings in comparison to bulk material and arc-sprayed coatings

Property	Cold spraying	AS	Bulk copper
Hardness, HV 0.3	130–150	90–100	125 (90% reduction in cross section)
Bond strength, MPa	10–20 (on steel)	~10 (on steel)	…
Electrical conductivity (at 20 °C, ref. bulk Cu)	60% (AS); 90% (1 h, 600 °C)	20% (AS); 40% (1 h, 600 °C)	100%

more rigid substrate materials require a longer incubation before successful coating formation (Ref 29, 30). That is attributed to the chemical activation of the substrate surfaces and the formation of certain local morphological arrangements for bonding by deformation. Both should also have an influence on bond strength. A major difference between cold-sprayed and AS Cu-coatings is in their electrical conductivities (Table 1). In the as-sprayed state, the cold-sprayed copper coatings already reach 60% of the conductivity of annealed bulk material, whereas the conductivity of the AS coating does not exceed 20%. By annealing at 600 °C, the conductivity of cold-sprayed copper coatings

can be improved to 90% with respect to annealed bulk material, a value not attainable by thermal spray coatings. The oxygen content of such cold-sprayed coatings of about 0.2% corresponds to that of the powder feedstock, whereas the oxygen content of the arc-sprayed coating of ~1.5% is significantly higher. In particular, the higher oxide content of the arc-sprayed coatings accounts for their poorer conductivity.

The first industrial applications of cold-sprayed copper coatings are used to improve the heat conductivity between electronic devices, an underlying copper plate and a soldered copper-coated heat sink, which is fabricated out of aluminum
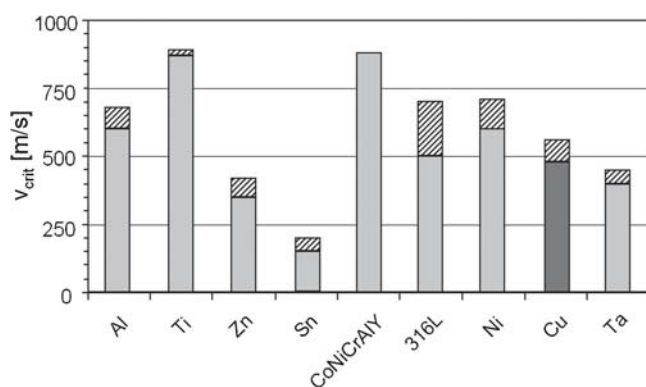
Fig. 9 Experimentally determined critical velocities of various spray materials. The error bar accounts for differences caused by the range of available powder purities.

(Ref 31). By using a cold-sprayed layer on the aluminum heat sink, a significantly higher and more uniform heat transfer can be guaranteed in comparison to that achieved with conventional brazing techniques or by using conventional thermal spraying to process the copper coating.

Figure 8 shows copper coating microstructures that were obtained by using a coarser powder ($-38 + 10$ μm), a MOC-designed nozzle (sintered WC-Co), and N_2 as the process gas at a gas inlet temperature of 500 °C and a pressure of 30 bar. The coating contains only a negligible amount of porosity, as demonstrated by Fig. 8(a). The results obtained by using identical conditions for etching to reveal the grain boundaries, as used for the coatings presented in Fig. 7(b), are illustrated in the close-up of Fig. 8(b). The comparison shows that higher velocities and higher process gas temperatures result in a higher degree of deformation inside former spray particles of copper coatings. With respect to coating quality, more interesting is the point that under these optimized process conditions most of the particle-particle interfaces appear in a similar contrast as normal grain boundaries. These results demonstrate that optimized nozzle designs improve not only the economy of the spray process but also the attainable coating qualities.

3.4 Application to Other Spray Materials

Using the procedure described in section 3.1, critical velocities for bonding in cold spraying were evaluated for different spray materials and are shown in Fig. 9. In the graph, different experimentally critical velocities are sorted in terms of spray material density. The comparison demonstrates that in materials of similar crystallographic structures (i.e., face-centered cubic) and stiffness (like aluminum and copper) density plays a role in bonding. Comparing hexagonal close-packed metals like Ti and Zn, it becomes obvious that such effects can be superimposed by a couple of other properties such as melting temperature or mechanical strength. The differences in critical velocities require subsequent tuning of the spray parameters for individual feedstock materials. The high critical velocities of the CiNiCrAlY and Ti powders show that such materials require the use of He as process gas to ensure bonding. More general attempts to quantify the different influences on critical velocity are given in re-
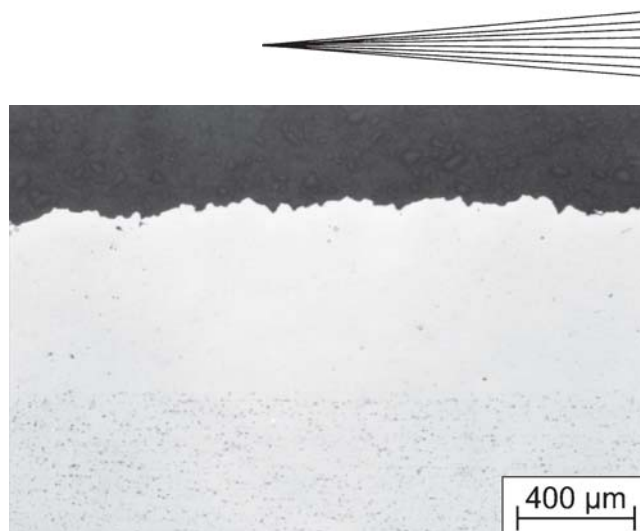
(a)
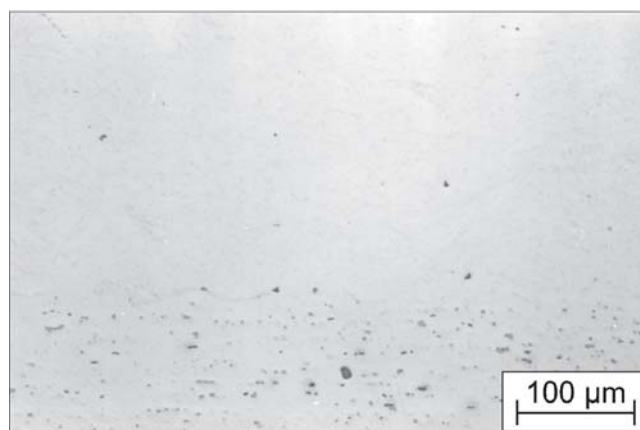
(b)

Fig. 10 Cold-sprayed Al 99.8 coating on an Al Mg3 substrate (powder -45 μm; MOC-designed nozzle for low-density materials; process gas N_2; temperature 250 °C; pressure 30 bar); (a) overview; (b) close-up

cently published investigations (Ref 21). In the present article, the different examples of coating microstructures represent just a snapshot of the coating types that are interesting for technical applications.

Consequently, strategies for optimizing cold spraying, as discussed in previous sections using the example of copper, were applied to other spray materials. The major aim of these investigations was to achieve optimum coating quality and high deposition efficiencies by using nitrogen as a process gas to reduce the costs of the possible applications. Only for spray materials that require substantially higher velocities for bonding, helium was used as the propellant medium. The following examples are aimed at demonstrating the versatility of cold spraying with respect to different feedstock materials.

Figure 10 shows microstructures that are attainable by cold spraying an aluminum coating (Al 99.8; in wt.%) on an AlMg3 substrate by using nitrogen as the process gas at a temperature of 250 °C and a nozzle that was MOC-designed especially for low-density materials. AlMg3 alloys were chosen as the substrate material to reveal the impacts on similar material and due to minimum efforts in substrate preparation. Oxide layers on aluminum sheets (the same conditions are valid for copper) are abraded in situ during the process by particles of lower velocity,

causing an erosion in the outer halo of the main particle stream. The coating is highly dense, and the interface to the substrate can be distinguished only by the presence of precipitates in the substrate. In the environment of artificial seawater, such aluminum coatings sprayed on magnesium substrates show the same corrosion potential as bulk aluminum sheets for a duration of more than 200 h (Fig. 11). As demonstrated for other less dense aluminum coatings during the process development, the oxygen corrosion in seawater will cause a drop down to the potential of the less noble component within minutes, as long as interconnecting porosity is present. Thus, such aluminum coatings can clearly be used for sacrificial corrosion protection and might also be of interest for avoiding the corrosion of less noble parts. Figure 12 shows typical micrographs of a stainless steel 316L coating that was sprayed on an aluminum substrate using a MOC-designed nozzle and nitrogen as the process gas (30 bar, 500 °C). Stainless steel 316L coatings can be tailored for pro-
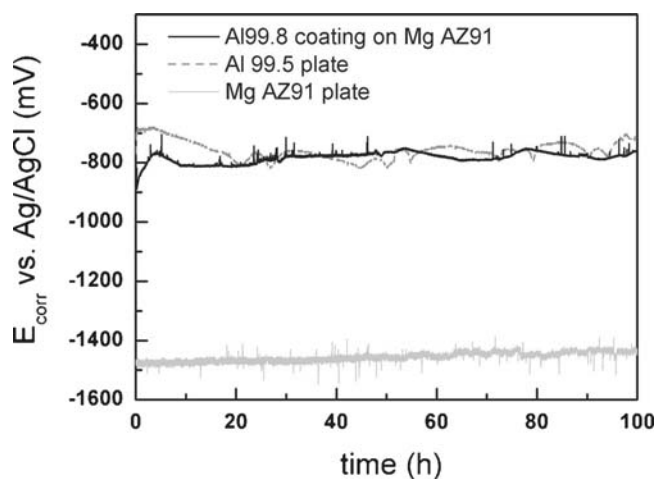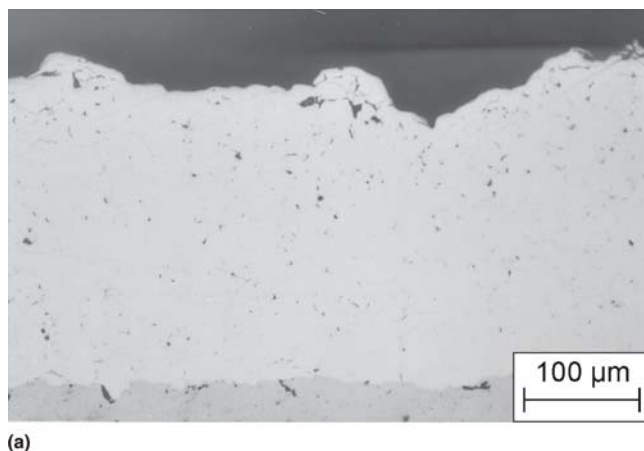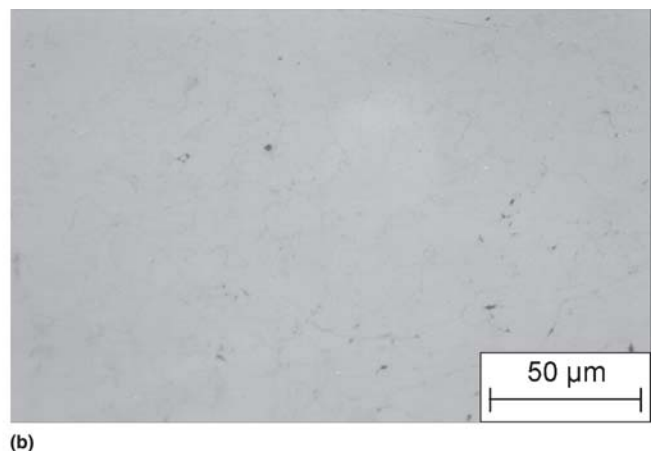
tection against wear and corrosion. Figure 13 shows the microstructure of a cold-sprayed CoNiCrAlY coating on a steel substrate. It is worth noting that the cold spraying of such high-strength CoNiCrAlY powders requires helium as a process gas and optimized MOC-designed nozzles due to the comparatively high critical velocity of this material. The possible application of cold-sprayed CoNiCrAlY coatings can be found in the field of high-temperature gas corrosion. Figure 14 demonstrates for the example of tantalum that even metals with very high melting temperatures are suitable as feedstock for cold spraying. The coating shown in Fig. 14 was processed with helium as process gas (MOC-designed nozzle, 25 bar, 300 °C). Despite the facts that the body-centered cubic structure of tantalum and the very high melting temperature might restrict possible deformation, coatings with low porosity can also be processed by using nitrogen as the process gas. The cold spraying of tantalum is of interest with respect to corrosion protection in acidic environments or in biomedical applications.

Figure 15 shows the microstructure of an aluminum-alumina ($Al-Al_2O_3$) composite coating that was processed by using a powder blend. Since spray conditions were chosen according to the parameters for pure aluminum (MOC-designed nozzle for low-density materials, N_2, 30 bar, 300 °C), the embedded hard phases demonstrate that the necessary conditions for bonding only have to be met by one of the involved spray materials. Such composites combine high electrical and thermal conductivity with enhanced wear resistance. Since the adhesion between ceramics and metals requires the activation of interfaces to ensure bonding, a substantial amount (50 vol.%) of the hard phase that is present in the powder blend is not incorporated into the coating. Nevertheless, it is worth noting that the embedded amount of about 15 vol.% of the hard phase already reduces two-body abrasive wear to half of that obtained for pure aluminum. In comparison to high-performance aluminum alloys, two-body wear is reduced by one third.

4. Conclusions

The present contribution demonstrates the current state of the art of cold spraying and the potential for process optimization.

Fig. 11 Corrosion potential (E_{corr}) of a cold-sprayed Al 99.8 coating on a Mg AZ 91 substrate compared to that of pure Al and the substrate material (powder −45 µm; MOC-designed nozzle for low-density materials; process gas N_2; temperature 250 °C; pressure 30 bar). The temporal evolution of E_{corr} demonstrates that even less noble substrates can be protected by cold-sprayed Al-coatings.

(a)

(b)

Fig. 12 Cold-sprayed 316L coating on an Al Mg3 substrate (powder −45 µm; MOC-designed, WC-Co nozzle; process gas N_2; temperature 500 °C; pressure 30 bar); (a) overview; (b) close-up

(a)

(b)

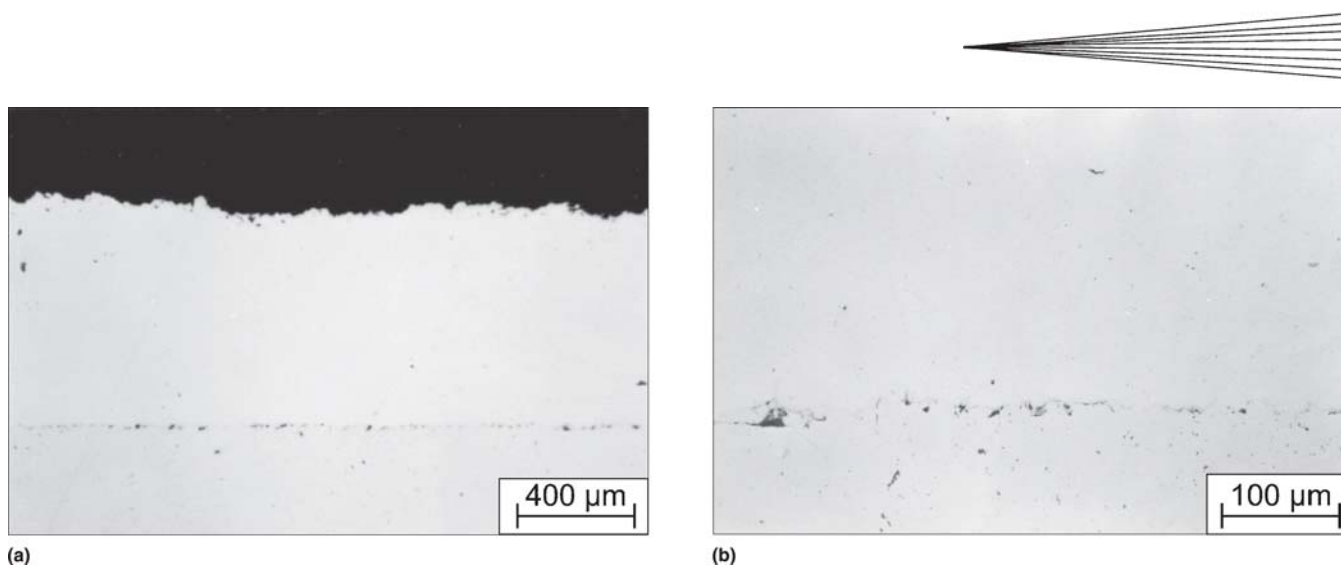**Fig. 13** Cold-sprayed CoNiCrAlY coating on a steel substrate (powder −45 μm; MOC-designed, WC-Co nozzle; process gas He; temperature 300 °C; pressure 25 bar); (a) overview; (b) close-up
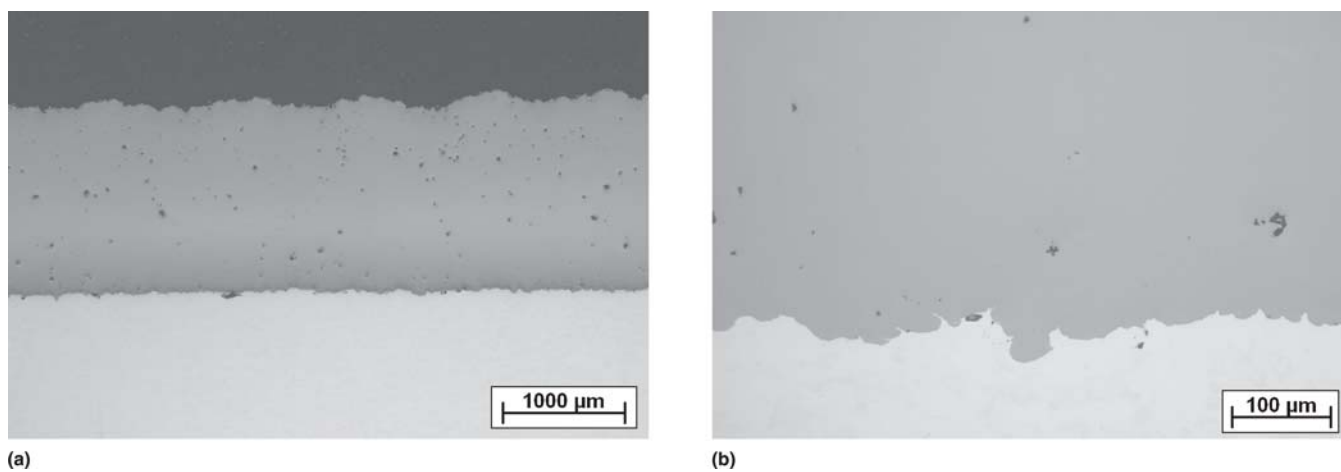

(a)

(b)

Fig. 14 Cold-sprayed Ta coating on a steel substrate (powder −45 μm; MOC-designed, WC-Co nozzle; process gas He; temperature 300 °C; pressure 25 bar); (a) overview; (b) close-up
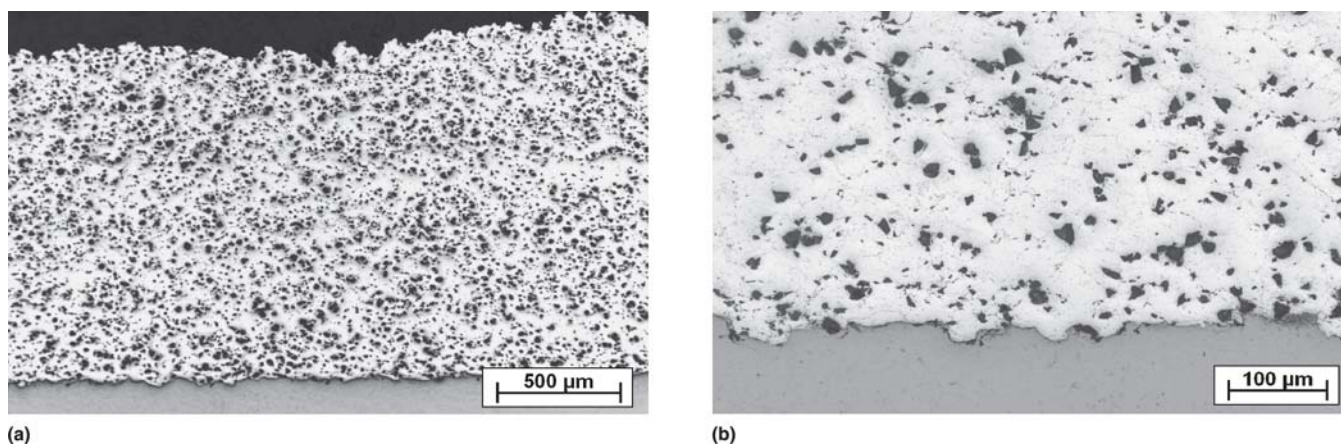

(a)

(b)

Fig. 15 Cold-sprayed Al-Al$_2$O$_3$ composite coating on a steel substrate (powder −45 μm; MOC-designed nozzle; process gas N$_2$; temperature 250 °C; pressure 30 bar); (a) overview; (b) close-up

As shown for the example of copper, cold-sprayed coatings can be processed with very low numbers of defects and low oxygen contents, and therefore exhibit bulklike properties with respect to electrical or thermal conductivity that are not attainable by normal thermal spray processes. The close link between the fundamental understanding of bonding mechanisms and fluid dynamics thereby proves to be a powerful tool for tuning cold spraying for various applications. Knowing the required conditions for bonding of a particular material, CFD can be used to predict the respective cold spray parameters. Moreover, fluid dynamics can be used for the design of optimized nozzle geometries, thus resulting in more economical process conditions and better coating qualities. The variety of materials that can be used in cold spraying demonstrate the manifold capabilities for technical applications.

Acknowledgment

References

1. H. Kreye, F. Gärtner, and H.J. Richter, High Velocity Oxy-Fuel Flame Spraying: State of the Art, New Developments and Alternatives, *Proc. 6. Kolloqium Hochgeschwindigkeits-Flammspritzen,* P. Heinrich, Ed., Gemeinschaft Thermisches Spritzen e.V., Unterschleißheim, Germany, 2003, p 5-17

2. A.P. Alkhimov, V.F. Kosarev, N.I. Nesterovich, and A.N. Papyrin, Method of Applying Coatings, Russian Patent 1618778, Sept 8, 1990, priority of the invention June 6, 1986

3. A.P. Alkhimov, A.N. Papyrin, V.F. Kosarev, N.I. Nesterovich, and M.M. Shushpanov, Gas-Dynamic Spray Method for Applying a Coating, U.S. Patent 5,302,414, April 12, 1994

4. A.P. Alkhimov, V.F. Kosarev, and A.N. Papyrin, A Method of Cold Gas-Dynamic Deposition, *Sov. Phys. Dokl.,* 1990, **35**(12), p 1047-1049 (Transl., American Inst. of Phys., 1991)

5. R.C. McCune and A.N. Papyrin, J.N. Hall, W.L. Riggs II, and P.H. Zajchowski, An Exploration of the Cold Gas-Dynamic Spray Method for Several Material Systems, *Advances in Thermal Spray Science and Technology,* C.C. Berndt and S. Sampath, Ed., Sept 11-15, 1995 (Houston, TX), ASM International, 1995, p 1-5

6. A.P. Alkhimov, S.V. Klinkov, V.F. Kosarev, and A.N. Paprin, Gas-Dynamic Spraying: Study of a Plane Supersonic Two Phase Jet, *J. Appl. Mech. Phys.,* 1997, **38**(2), p 176-183

7. T. Stoltenhoff, H. Kreye, and H.J. Richter, An Analysis of the Cold Spray Process and Its Coatings, *J. Thermal Spray Technol.,* 2002, **11,** p 542-550

8. T.H. Van Steenkiste, Kinetic Spraying: A New Coating Proess, *Key Eng. Mater.,* 2001, **197**, p 59-85

9. T.H. Van Steenkiste and J.R. Smith, Evaluation of Coatings Produced via Kinetic and Cold Spray Processes, *J. Thermal Spray Technol.,* 2004, **13**(2), p 274-282

10. A.I. Kashirin, O.F. Klyuev, and T.V. Buzdygar, Apparatus for Gas-Dynamic Coating, U.S. Patent 6,402,050 B1, June 11, 2002

11. H. Gabel and R.M. Tapphorn, A Apparatus and Process for Solid-State Deposition and Consolidation of High Velocity Powder Particles using Thermal Plastic Deformation, W.O. Patent 02-085332 A1, October 21, 2002

12. D.L. Gilmore, R.C. Dykhuizen, R.A. Neiser, T.J. Roemer, and M.F. Smith, Particle Velocity and Deposition Efficiency in the Cold Spray Process, *J. Thermal Spray Technol.,* 1999, **8**(4), p 576-582

13. A. Papyrin, Cold Spray Technology, *Adv. Mater. Proc.,* 2001, **159**(9), p 49-51

14. J. Voyer, T. Stoltenhoff, T. Schmidt, Method and Potential of the Cold Spray Process, *Proc. 6. Kolloqium Hochgeschwindigkeits-Flammspritzen,* P. Heinrich, Ed., Gemeinschaft Thermisches Spritzen e.V., Unterschleißheim, Germany, 2003, p 39-47

15. M. Grujicic, C.L. Zhao, C. Tong, W.S. DeRosset, and D. Helfritch, Analysis of the impact Velocity of Powder Particles in the Cold-Gas Dynamic-Spray Process, *Mater. Sci. Eng., A,* 2003, **368**(1-2), p 222-230

16. W.Y. Li and C.J. Li, Optimal Design of a Novel Cold Spray Gun Nozzle at a Limited Space, *J. Thermal Spray Technol.,* 2005, **14**(3), p 391-396

17. R.C. Dykhuisen, M.F. Smith, D.L. Gilmore, R.A. Neiser, X. Jiang, and S. Sampath, Impact of Hgh Velocity Cold Spray Particles, *J. Thermal Spray Technol.,* 1999, **8**(4), p 559-564

18. H. Assadi, F. Gärtner, T. Stoltenhoff, and H. Kreye, Bonding Mechanism in Cold Gas Spraying, *Acta Mater.,* 2003, **51**, p 4379-4394

19. M. Grujicic, C.L. Zhao, W.S. DeRosset, and D. Helfritch, Adiabatic Shear Instability Based Mechanism for Partcles/Substrate Bonding in the Cold-Gad Dynamic-Spray Process, *Mater. Des.,* 2004, **25**(8), p 681-688

20. C.J. Li and W.-Y. Li, Examination of the Critical Velocity for Deposition of Particles in Cold Spraying, *Thermal Spray Connects: Explore Its Surfacing Potential,* E. Lugscheider, Ed., May 2-4, 2005 (Basel, Switzerland), DVS Deutscher Verband für Schweißen, 2005, p 217-224

21. T. Schmidt, F. Gärtner, H. Assadi, and H. Kreye, Development of a Generalized Parameter Window for Cold Spray Deposition, *Acta Mater.,* 2006, **54**(3), p 729-742

22. L. Ajdelsztajn, B. Jodoin, G.E. Kim, and J.M. Schoeung, Cold Spray Deposition of Nanocrystalline Aluminum Alloys, *Metall. Mater. Trans. A*, 2005, **36**(3), p 657-666

23. R.S. Lima, J. Karthikeyan, C.M. Kay, J. Lindemann, and C.C. Berndt, Microstructural Characteristics of Cold-Sprayed Nanostructured WC-Co Coatings, *Thin Solid Films,* 2002, **416**(1-2), p 129-135

24. H.J. Kim, C.H. Lee, and S.Y. Hwang, Superhard Nano WC- 12 %Co Coating by Cold Spray Deposition, *Mater. Sci. Eng., A,* 2005, **391**(1-2), p 243-248

25. S. Yoon, H.J. Kim, and C.H. Lee, Deposition Behaviour of Bulk Amorphous NiTiZrSiSn According to the Kinetic and Thermal Energy Levels in the Kinetic Spray Process, *Surf. Coat. Technol.,* 2006, **200,** p 6022-6029

26. Standard Test Method for Adhesion or Cohesion Strength of Thermal Spray Coatings, C 633-01, *Annual Book of ASTM Standards,* ASTM, 2001

27. P. Heinrich, H. Kreye, and T. Stoltenhoff, Laval Nozzle for Thermal and Kinetic Spraying, U.S. Patent 2005/0001075 A1, January 6, 2005

28. J. Karthikeyan, International Status of Cold Spray Technology, *Spraytime,* 2005, **12**(1), p 1-4

29. A.N. Papyrin, S.V. Klinkov, and V.F. Kosarev, Effect of the Substrate Surface Activation on the Process of Cold Spray Coating Formation, *Thermal Spray Connects: Explore Its Surfacing Potential,* E. Lugscheider, Ed., May 2-4, 2005 (Basel, Switzerland), DVS Deutscher Verband für Schweißen, 2005, p 145-150

30. S.V. Klinkov, V.F. Kosarev, M. Rein, Cold Spray Deposition: Significance of Particle Impact Phenomena, *Aerospace Sci. Technol.,* **9** (7), p 582-591

31. D. Grasme, First Serial Application of Cold Spraying for Coating Heat Sinks, *Proc. 6 Kolloqium Hochgeschwindigkeits-Flammspritzen* (Unterschleißheim, Germany), P. Heinrich, Ed., Gemeinschaft Thermisches Spritzen e.V., 2003, p 119-122